

# Effect of Nickel Oxide on Morphological and Electrical Properties of Manganese Oxide Nanostructured Thin Films

Ali Younis Ibrahim and Faisal Ghazi Hammoodi

*Department of Physics, College of Science, University of Diyala, 32001 Baqubah, Diyala, Iraq  
{ywns1764, faslgaze}@gmail.com*

**Keywords:** Mn<sub>3</sub>O<sub>4</sub> Film, Hall Effect, FE-SE, Doping Effect, EDS.

**Abstract:** In this study, thin films of manganese oxide (Mn<sub>3</sub>O<sub>4</sub>) doped with nickel oxide (NiO) at different doping ratios (0, 1, 3, 5, and 7%) were prepared and deposited on glass slides at a temperature of 350°C using the chemical spray pyrolysis technique. Spectral analysis was performed, and a scanning electron microscope (SEM) was used. The SEM results show that the prepared films are spherical in shape, resembling cauliflower, and are irregular in size. This irregularity is due to the crystalline defects generated in the films. An Energy Dispersive Spectrometer (EDS) analysis was conducted to verify the components of the prepared thin films, which allowed for the determination of the weight and atomic ratios of the elements composing the films. Regarding the electrical measurements, conductivity, resistivity, the Hall coefficient, and charge carrier concentration were determined. We note that the prepared films exhibit p-type charge carriers and that the Hall effect increases with increasing doping ratios. The Hall coefficient values increase with doping ratios and reach their highest value at 3%, while the resistivity values peak at a doping ratio of 1%. The films show low conductivity overall, with the highest conductivity value observed at 7% doping. Similarly, the mobility increases with doping and attains its highest value at 7%.

## 1 INTRODUCTION

The advancement of nano science, an interdisciplinary field encompassing physics, chemistry, and material science, has recently been greatly aided by nanostructured thin films. [1], Manganese oxides are becoming one of the most potent transition metal oxides and diverse classes of functional materials that are having a key impact on science and technology [2], [3] , Manganese (Mn) is a metallic element belonging to Group 7 in the periodic table of elements and is known for its distinctive mineral and chemical properties. Manganese chloride occurs naturally in the environment, but it can also be prepared in the laboratory or by industrial means. It is typically available as a white powder or crystalline crystals and is soluble in water. Thin films are thin layers of materials used in semiconductor technology and electronic devices [4] , Manganese oxides, which are magnetic by nature, can form various crystal structures like MnO, Mn<sub>2</sub>O<sub>3</sub>, Mn<sub>3</sub>O<sub>4</sub>, and others, and exhibit various oxidation states of manganese, such as Mn<sup>2+</sup>, Mn<sup>3+</sup>, or Mn<sup>4+</sup> [5] , p-type change Metal oxides are of great interest because of their

participation in a variety of applications, including photovoltaic solar cells, electrochemical energy storage devices, microelectronic devices, and metal-oxide-semiconductor field-effect transistors (p MOSFETs) [6]-[9] , Nickel oxide (NiO) is a crystalline powder, either green or black in color, with density 6.67 g/cm<sup>3</sup>, molecular weight 842.87 g/mol, and melting point 1984 C<sup>0</sup> [10] Nickel oxide (NiO) is non-insulating at room temperature and is an antiferromagnetic material with good resistance. It also has a large energy gap estimated at 3.4 - 4 eV and is considered one of the important electrolytic materials after tungsten oxide. It is used in making the electric anode and has several uses due to the high electrolytic efficiency. Nickel oxide has high stability and has positive conductivity [11], A variety of techniques have been used to grow manganese oxide thin films such as chemical bath deposition [12], [13] , dip coat [14] electrochemical deposition [15] , atomic layer deposition [16] , electrostatic spray deposition [17], pulsed laser deposition [18], chemical vapor deposition [19] and SILAR method [20] chemical pyrolysis technique [21], Because it is easy to use, inexpensive, and produces little waste, spray

pyrolysis is a good substitute for conventional methods for creating manganese oxide thin films. It can be applied to a wide surface area and is simple to integrate into an industrial production line. This method works with mass production systems as well [22]

## 2 EXPERIMENTAL PART

Chemical spray pyrolysis (CSP) method was employed to create thin films of manganese oxide ( $\text{Mn}_3\text{O}_4$ ) doped with nickel oxide (NiO). German-made glass plates from Los Las Company were prepared. The plates were cut into ( $2.5 \times 2.5$ ) cm dimensions and rinsed with distilled water for 4 minutes in an ultrasonic device. After that, they were sterilized with acetone for 4 minutes and then again with distilled water. Finally, they were dried with a special fabric to remove the remaining suspended particles. The oxide solution was prepared by mixing manganese chloride ( $\text{MnCl}_2 \cdot 4\text{H}_2\text{O}$ ) weighing 1.979 g in 100 ml of distilled water. Then, it was placed on a magnetic stirrer for 10 minutes. Then, it was filtered using filter paper. After that, it was deposited using a spray system on the glass plates at a temperature of  $350^\circ\text{C}$ . The pure oxide films were doped with nickel oxide at ratios of 0%, 1%, 3%, 5% and 7% . The effect of Hall measurements was studied to determine the efficiency of the semiconductor using an HMS 300 device, This device operates based on the Van Der Pauw method and is connected to a computer equipped with software that displays the important parameters of the sample under examination, such as the type of

semiconductor, carrier concentration, mobility, and Hall coefficient , The produced films' surface morphology was also examined using a Field Emission Scanning Electron Microscope (FE-SEM) of the MIRA3, Model-TE-SCAN type, located at the University of Tehran, Islamic Republic of Iran. The FE-SEM device enables the determination of particle shape, homogeneity, as well as the detection of crystalline structure defects

## 3 RESULT AND DISCUSSION

### 3.1 Results of Field Emission Scanning Electron Microscopy Tests

Field-emitting scanning electron microscopy (FE SEM) is used to examine the surface topography of all the prepared membranes was studied at a temperature of  $350^\circ\text{C}$ . This device gives a structural image of the surface with very high accuracy. Figures 1a, 1b, 1d, 1e show FE SEM images and cross sections of the prepared films. It is formed in beautiful shapes, spherical shapes gathered in the form of a flower very similar to a cauliflower flower. It is also irregular in size and distribution and uneven in growth, noting the presence of voids resulting from the occurrence of secondary growth as well as due to crystalline defects. We note that the average crystal size has large differences due to the lack of good homogeneity of the membranes [23], [24] .

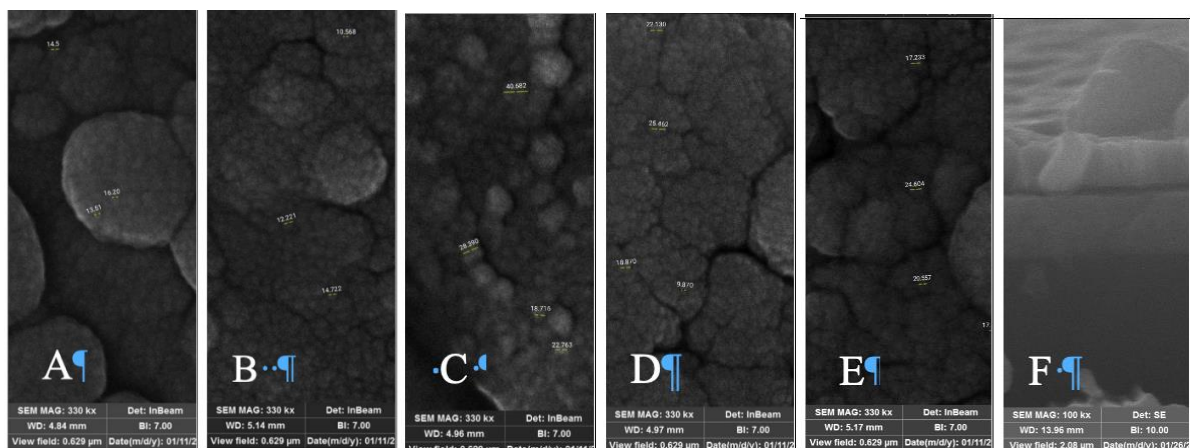


Figure 1: FE-SEM Images of : a)  $\text{Mn}_3\text{O}_4$ : Pure, b)  $\text{Mn}_3\text{O}_4$ : NiO (1%), c)  $\text{Mn}_3\text{O}_4$ : NiO (3%), d)  $\text{Mn}_3\text{O}_4$ : NiO (5%), e)  $\text{Mn}_3\text{O}_4$ : NiO (7%), f) Cross-sectional view showing the film thickness ( $\sim 327$  nm).

We observe that the  $\text{Mn}_3\text{O}_4$  membrane with a 7% impurity rate had the biggest particle size, whereas the membrane with a 1% nickel oxide impurity rate had the lowest value. As seen in Figure 1f, the produced film layer has a thickness of roughly 327 nm.

### 3.2 Results of Energy Dispersive Spectrometer Test

To verify the components of the prepared thin films, we conduct an examination Energy Dispersive Spectrometer (EDS), which is an examination through which the weight percentages and atomic percentages of the elements present in the prepared films that cannot be detected using X-ray technology (XRD). The following Figures 2, 3, 4, 5, 6 are diagrams showing the analysis of EDS and the following Tables 1, 2, 3, 4, 5 show the weight percentages and atomic percentages of the elements present in the prepared films.

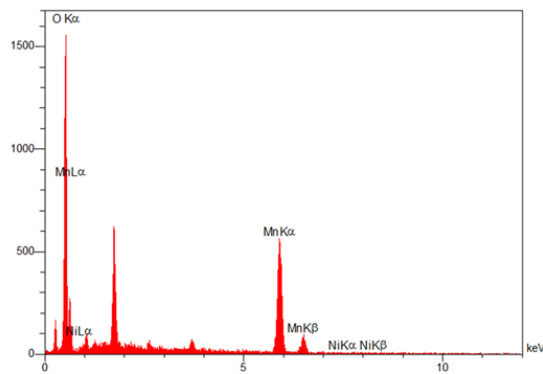


Figure 2: Analysis diagram EDS for a thin  $\text{Mn}_3\text{O}_4$  film.

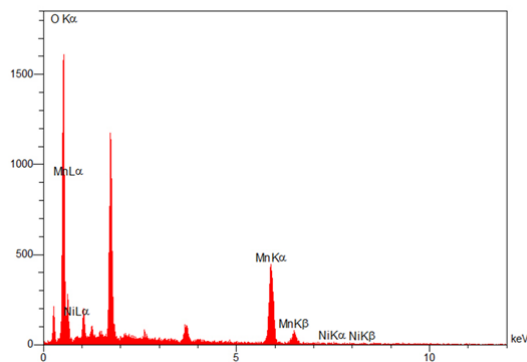


Figure 3: Analysis diagram EDS for a thin  $\text{Mn}_3\text{O}_4$  film.

Table 1: Weight ratios and atomic ratios of elements in the film  $\text{Mn}_3\text{O}_4$  for analysis EDS.

| Element | Weight (%) | Atomic (%) |
|---------|------------|------------|
| O       | 47.89      | 75.94      |
| Mn      | 51.88      | 23.96      |
| Ni      | 0.23       | 0.10       |

Table 2: Weight ratios and atomic ratios of elements in the film  $\text{Mn}_3\text{O}_4$  for analysis EDS.

| Element | Weight (%) | Atomic (%) |
|---------|------------|------------|
| O       | 54.64      | 80.54      |
| Mn      | 45.00      | 19.32      |
| Ni      | 0.35       | 0.14       |

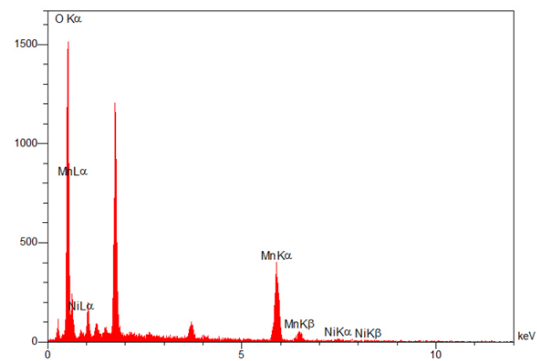


Figure 4: Analysis diagram EDS for a thin  $\text{Mn}_3\text{O}_4$  film.

Table 3: Weight ratios and atomic ratios of elements in the film  $\text{Mn}_3\text{O}_4$  for analysis EDS.

| Element | Weight (%) | Atomic (%) |
|---------|------------|------------|
| O       | 57.60      | 82.37      |
| Mn      | 41.55      | 17.30      |
| Ni      | 0.85       | 0.33       |

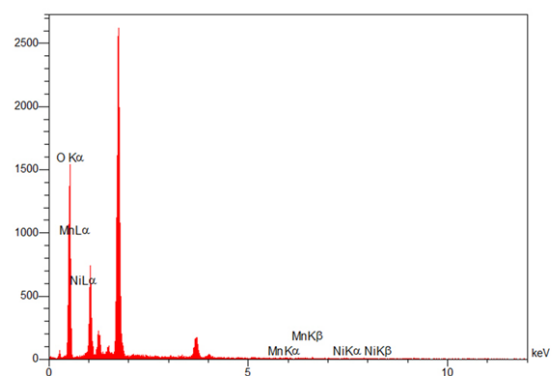


Figure 5: Analysis diagram EDS for a thin  $\text{Mn}_3\text{O}_4$  film.

Table 4: Weight ratios and atomic ratios of elements in the film  $Mn_3O_4$  for analysis EDS.

| Element | Weight (%) | Atomic (%) |
|---------|------------|------------|
| O       | 98.92      | 99.70      |
| Mn      | 0.42       | 0.12       |
| Ni      | 0.65       | 0.18       |

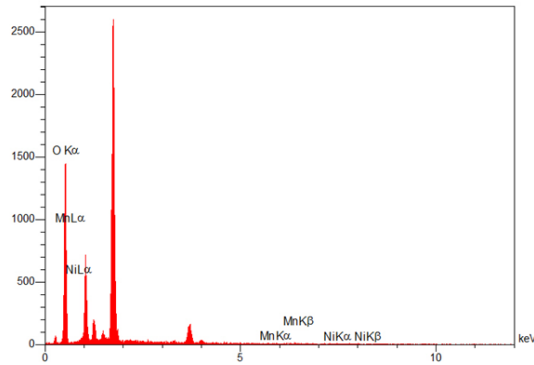

 Figure 6: Analysis diagram EDS for a thin  $Mn_3O_4$  film.

 Table 5: Weight ratios and atomic ratios of elements in the film  $Mn_3O_4$  for analysis EDS.

| Element | Weight (%) | Atomic (%) |
|---------|------------|------------|
| O       | 98.70      | 99.63      |
| Mn      | 0.57       | 0.17       |
| Ni      | 0.73       | 0.20       |

### 3.3 Results of Electrical Measurement

The Hall effect was conducted as a measurement to determine the electrical characteristics of  $Mn_3O_4$  films made at  $350\text{ }^{\circ}\text{C}$  and with impurity rates 0%,

1%, 3%, 5% and 7 % of nickel oxide. Through it the important electrical properties were known, such as the type of charge carriers, their concentration, and the values of the Hall coefficient. It is found that all the prepared  $Mn_3O_4$  due to positive Hall coefficient values, which indicate that holes make up the majority of charge carriers and electrons make up the minority, membranes are of the positive type (P-type) [25] , Table 6 shows the results of the Hall effect , We notice that the values of the effect of the Hall coefficient increase with increasing doping rates, and its highest value is at a doping percentage of 3% of nickel oxide , The results show that the resistivity values of all the prepared films are high, and their highest value occurs at a doping rate of 1% of nickel oxide. The reason for the high resistivity values is the crystalline defects resulting from Ni ions, as they restrict the movement of electrons and increase their resistance [26]. All produced membranes had low conductivity values , as we note that they increased after the doping process with nickel oxide, and their highest value was at the doping rate of 7% of nickel oxide ,The reason for the increase in conductivity is the replacement of  $Mn_3O_4$  with  $NiO$  ions, which gives the electrons increased freedom and leads to an increase in electrical conductivity [27], [28]. The mobility increases with increasing doping rates, and its highest value was at a doping percentage of 7% of nickel oxide, Figures 7, 8, 9 shows the values of resistivity , Hall coefficient , and charge carrier concentration as a function of doping ratios, respectively, for all prepared films.

Table 6: Hall effect measurements for the prepared thin films.

| Sample               | Concentration $(\text{cm}^{-3})$ | Hall Coefficient RH $(\text{m}^2/\text{C})$ | Conductivity $(\Omega.\text{cm})^{-1}$ | Resistivity $(\Omega.\text{cm})$ | Mobility $(\text{cm}^2/\text{v.s})$ |
|----------------------|----------------------------------|---|--|----------------------------------|-------------------------------------|
| Pure                 | $2.025 \times 10^{11}$           | $3.082 \times 10^7$                         | $0.772 \times 10^{-5}$                 | $12.98 \times 10^4$              | $2.374 \times 10^2$                 |
| $Mn_3O_4$ : NiO (1%) | $2.748 \times 10^{11}$           | $2.271 \times 10^7$                         | $0.523 \times 10^{-5}$                 | $19.15 \times 10^4$              | $1.186 \times 10^2$                 |
| $Mn_3O_4$ : NiO (3%) | $10.52 \times 10^{11}$           | $0.5934 \times 10^7$                        | $2.017 \times 10^{-5}$                 | $4.829 \times 10^4$              | $1.229 \times 10^2$                 |
| $Mn_3O_4$ : NiO (5%) | $1.912 \times 10^{11}$           | $3.265 \times 10^7$                         | $1.247 \times 10^{-5}$                 | $8.016 \times 10^4$              | $4.073 \times 10^2$                 |
| $Mn_3O_4$ : NiO (7%) | $2.014 \times 10^{11}$           | $3.100 \times 10^7$                         | $1.614 \times 10^{-5}$                 | $6.198 \times 10^4$              | $5.002 \times 10^2$                 |

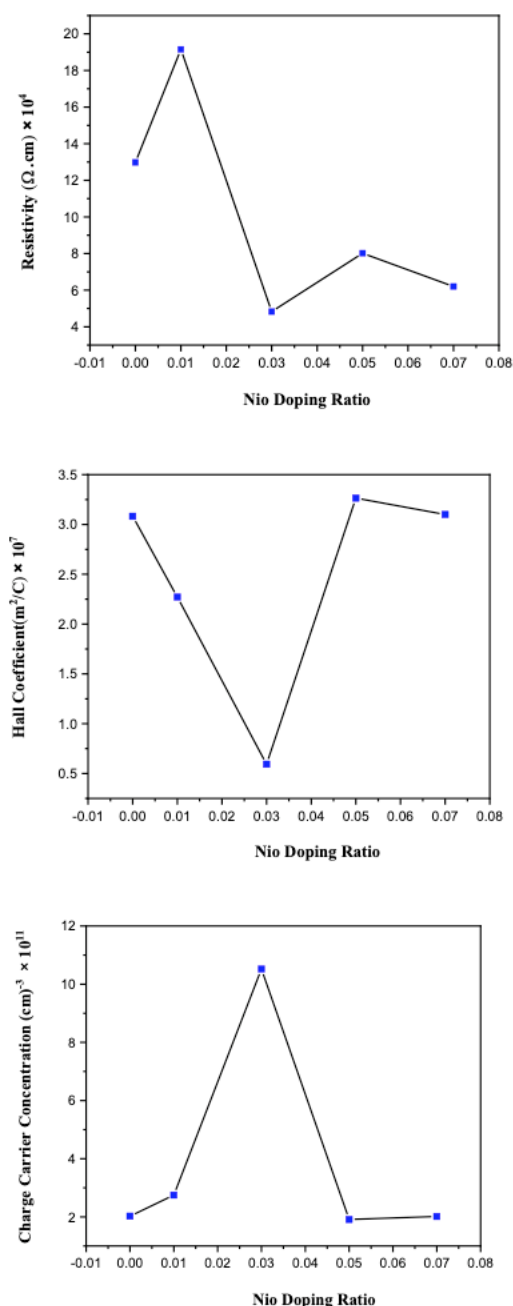


Figure 9: Concentration of charge carriers as a function of doping ratios for the prepared films.

## 4 CONCLUSIONS

This study demonstrates that NiO doping has a significant impact on the morphological and electrical properties of  $\text{Mn}_3\text{O}_4$  nanostructured thin films. SEM analysis revealed a cauliflower-like,

spherical morphology and pronounced size irregularity, attributed to crystalline defects—the largest particle size was observed at 7% NiO content. EDS confirmed the presence of Mn, O, and Ni, with manganese concentration declining and nickel peaking at intermediate doping levels.

Electrical measurements showed all films exhibit p-type conductivity. The Hall coefficient reached its maximum at 3% NiO, while resistivity peaked at 1% doping and conductivity and carrier mobility were highest at 7% NiO. These trends indicate that controlled NiO doping efficiently tailors film properties, with optimal electrical characteristics achieved at specific doping ratios. Overall, the findings support the use of NiO doping to optimize  $\text{Mn}_3\text{O}_4$  thin films for applications in electronic and energy devices.

## REFERENCES

- [1] M. Belkhedkar and A. Ubale, "Physical properties of nanostructured  $\text{Mn}_3\text{O}_4$  thin films synthesized by SILAR method at room temperature for antibacterial application," *J. Mol. Struct.*, vol. 1068, pp. 94-100, 2014.
- [2] M. He, L. Kang, C. Liu, Z. Lei, and Z.-H. Liu, "Layer-by-layer assembly of manganese-cobalt-nickel oxide nanosheets/graphene composite films," *Mater. Res. Bull.*, vol. 68, pp. 194-202, 2015.
- [3] V. Štengl, J. Bludská, F. Opluštil, and T. Němec, "Mesoporous titanium-manganese dioxide for sulphur mustard and soman decontamination," *Mater. Res. Bull.*, vol. 46, no. 11, pp. 2050-2056, 2011.
- [4] H. S. Al-Rikabi, M. H. Al-Timimi, and I. K. Abd, "A review of (MgO) thin films, preparation and applications," in *AIP Conf. Proc.*, vol. 2834, no. 1, AIP Publishing, 2023.
- [5] V. Pandey, S. Munjal, and T. Ahmad, "Optical properties and spectroscopic investigation of single phase tetragonal  $\text{Mn}_3\text{O}_4$  nanoparticles," *Mater. Today Proc.*, vol. 26, pp. 1181-1183, 2020.
- [6] N. M. Karim, S. Manzoor, and N. Soin, "Unification of contemporary negative bias temperature instability models for p-MOSFET energy degradation," *Renew. Sustain. Energy Rev.*, vol. 26, pp. 776-780, 2013.
- [7] H.-K. Rhee, I.-S. Nam, and J. M. Park, *New Developments and Application in Chemical Reaction Engineering: Proc. of the 4th Asia-Pacific Chemical Reaction Engineering Symp. (APCRE'05)*, Gyeongju, Korea, Jun. 12–15, 2005. Elsevier, 2006.
- [8] W. Suprun, M. Lutecki, R. Gläser, and H. Papp, "Catalytic activity of bifunctional transition metal oxide containing phosphated alumina catalysts in the dehydration of glycerol," *J. Mol. Catal. A Chem.*, vol. 342, pp. 91-100, 2011.
- [9] I. Kuznetsov, M. Greenfield, Y. Mehta, W. Merchan-Merchan, G. Salkar, and A. Saveliev, "Increasing the solar cell power output by coating with transition metal-oxide nanorods," *Appl. Energy*, vol. 88, no. 11, pp. 4218-4221, 2011.

- [10] F. Saadati, A. Grayeli, and H. Savaloni, "Dependence of the optical properties of NiO thin films on film thickness and nano-structure," 2010.
- [11] P. Patil and L. Kadam, "Preparation and characterization of spray pyrolyzed nickel oxide (NiO) thin films," *Appl. Surf. Sci.*, vol. 199, no. 1-4, pp. 211-221, 2002.
- [12] D. Dubal, D. Dhawale, R. Salunkhe, V. Fulari, and C. Lokhande, "Chemical synthesis and characterization of  $\text{Mn}_3\text{O}_4$  thin films for supercapacitor application," *J. Alloys Compd.*, vol. 497, no. 1-2, pp. 166-170, 2010.
- [13] H. Y. Xu, S. L. Xu, X. D. Li, H. Wang, and H. Yan, "Chemical bath deposition of hausmannite  $\text{Mn}_3\text{O}_4$  thin films," *Appl. Surf. Sci.*, vol. 252, no. 12, pp. 4091-4096, 2006.
- [14] S. C. Pang, M. A. Anderson, and T. W. Chapman, "Novel electrode materials for thin-film ultracapacitors: comparison of electrochemical properties of sol-gel-derived and electrodeposited manganese dioxide," *J. Electrochem. Soc.*, vol. 147, no. 2, p. 444, 2000.
- [15] C.-C. Hu and T.-W. Tsou, "Ideal capacitive behavior of hydrous manganese oxide prepared by anodic deposition," *Electrochem. Commun.*, vol. 4, no. 2, pp. 105-109, 2002.
- [16] O. Nilsen, H. Fjellvåg, and A. Kjekshus, "Growth of manganese oxide thin films by atomic layer deposition," *Thin Solid Films*, vol. 444, no. 1-2, pp. 44-51, 2003.
- [17] Y. Dai, K. Wang, J. Zhao, and J. Xie, "Manganese oxide film electrodes prepared by electrostatic spray deposition for electrochemical capacitors from the  $\text{KMnO}_4$  solution," *J. Power Sources*, vol. 161, no. 1, pp. 737-742, 2006.
- [18] S. Isber, E. Majdalani, M. Tabbal, T. Christidis, K. Zahraman, and B. Nsouli, "Study of manganese oxide thin films grown by pulsed laser deposition," *Thin Solid Films*, vol. 517, no. 5, pp. 1592-1595, 2009.
- [19] T. Maruyama and S. Arai, "Electrochromic properties of cobalt oxide thin films prepared by chemical vapor deposition," *J. Electrochem. Soc.*, vol. 143, no. 4, p. 1383, 1996.
- [20] A. Ubale, M. Belkhedkar, Y. Sakhare, A. Singh, C. Gurada, and D. Kothari, "Characterization of nanostructured  $\text{Mn}_3\text{O}_4$  thin films grown by SILAR method at room temperature," *Mater. Chem. Phys.*, vol. 136, no. 2-3, pp. 1067-1072, 2012.
- [21] A. M. Shano, A. A. Habeeb, Z. T. Khodair, and S. K. Adnan, "Effects of thickness on the structural and optical properties of  $\text{Mn}_3\text{O}_4$  nanostructure thin films," in *J. Phys. Conf. Ser.*, vol. 1818, no. 1, p. 012049, 2021.
- [22] M. H. Abdul-Allah, F. A. Ahmed, and F. G. Hammody, "Influence of gamma radiation on optical properties of  $(\text{Mn}_2\text{O}_3)_{1-x}(\text{CuO})_x$  films," 2014.
- [23] N. A. Bakr, "Studies on structural, optical and electrical properties of hydrogenated nanocrystalline silicon (nc-Si:H) thin films grown by hot wire-CVD for photovoltaic applications," 2010.
- [24] M. Hakimi, H. A. Hosseini, and B. Elhaminezhad, "Fabrication of manganese dioxide nanoparticles in starch and gelatin beds: investigation of photocatalytic activity," *Chem. Methodol.*, vol. 8, pp. 37-46, 2024.
- [25] R. R. Prabhakar et al., "Facile water-based spray pyrolysis of earth-abundant  $\text{Cu}_2\text{FeSnS}_4$  thin films as an efficient counter electrode in dye-sensitized solar cells," *ACS Appl. Mater. Interfaces*, vol. 6, no. 20, pp. 17661-17667, 2014.
- [26] C. Coughlan, M. Ibanez, O. Dobrozhan, A. Singh, A. Cabot, and K. M. Ryan, "Compound copper chalcogenide nanocrystals," *Chem. Rev.*, vol. 117, no. 9, pp. 5865-6109, 2017.
- [27] A. Hosseinian, A. R. Mahjoub, and M. Movahedi, "Low temperature synthesis and characterization of nanocrystalline CdO film by using a solvothermal method without any additives," 2010.
- [28] G. Turgut, "An investigation of Pb-contribution effect on the characteristic features of CdO films coated with a sol-gel spin coating technique," *J. Mater. Sci. Mater. Electron.*, vol. 28, no. 22, pp. 16992-17001, 2017.